IEEE Access
Multidisciplinary : Rapid Review : Open Access Journal

Received August 29, 2019, accepted September 18, 2019, date of publication October 3, 2019, date of current version October 21, 2019.

Digital Object Identifier 10.1109/ACCESS.2019.2945357

Multipath Based Adaptive Concurrent Transfer for Real-Time Video Streaming Over 5G Multi-RAT Systems

SOOEUN SONG[1], JAEWOOK JUNG[1], MINSU CHOI[1], CHANGSUNG LEE[1], JUNGKYU SUN[2,3], AND JONG-MOON CHUNG[1,3], (Senior Member, IEEE)

[1]School of Electrical and Electronic Engineering, Yonsei University, Seoul 03722, South Korea
[2]LIG Nex1 Company Ltd., Seongnam 13488, South Korea
[3]Department of Defense Fusion Engineering, Yonsei University, Seoul 03722, South Korea

Corresponding author: Jong-Moon Chung (jmc@yonsei.ac.kr)

This work was supported by LIG Nex1 Company Ltd.

ABSTRACT 5G systems use multiple radio access technology (multi-RAT) to provide broadband, low latency, and high reliability services. Multi-RAT is effective when multipath transmission is used over multichannels. This is why multipath based transmission is one of the key technologies that can improve the throughput and reliability of real-time video streaming over 5G networks. This paper proposes two multipath based concurrent transfer techniques; fast concurrent transfer (FCT) and reliable concurrent transfer (RCT). FCT aims to minimize the round trip time (RTT) required for frame transmission by arranging each of the packets constituting a frame to be sent over multiple channels. In an environment where there are multiple channels, RCT performs redundant transmission of packets, so that even if a packet is lost in one path, the lost packet can be received safely over another path. FCT aims at securing the reliability of data transmission. In addition, a multipath based adaptive concurrent transmission (MACT) scheme is proposed which controls the ratio of FCT and RCT adaptively considering the state of the receiver buffer, inflow throughput, and decoding rate to enhance the reliability and throughput performance. The simulation results show that the proposed MACT scheme results in a better performance compared to the conventional transmission schemes in various network channel conditions.

INDEX TERMS Real-time video streaming, wireless networks, multipath UDP, H.264.

I. INTRODUCTION

The fifth generation (5G) networks are projected to support various real-time vision-based services, like augmented reality (AR), virtual reality (VR), and remote control services, such as, autonomous driving of connected cars and remote surgery [1]. Vision-based intelligent real-time services used in supporting safety critical operations require more strict constraints, such as, high reliability, low latency, and high resolution video. For example, eHealth, unmanned and remote-controlled vehicles require latency less than tens to hundreds of milliseconds with reliability exceeding 99% [1]. As these examples show, the importance of video streaming applications in 5G networks is significant.

Many vision-based intelligent services are targeted for robots and unmanned vehicles in which wireless networking is essential. However, wireless networks can experience very high packet loss rates (PLRs) due to fading, shadowing fluctuation, and inter-cell interference [2]. Packet losses in real-time video transfer results in stalling during play, which is critical to the video's quality of experience (QoE). In addition, PLR variations make real-time video transfer across wireless networks very challenging [3]. 5G wireless networks are being designed to comprise and utilize multi-radio access technologies (multi-RATs) to achieve high capacity, high QoE, and low latency [4]. Recent mobile devices already include multiple wireless interfaces to receive data simultaneously over multiple wireless networks, such as 5G, LTE, and Wi-Fi [5]. This enables multihoming, allowing connections between the two endpoints via multiple IP addresses or network interface cards.

Multipath transmission schemes have emerged as technologies that can help to enhance the reliability and throughput of wireless networks. Multipath techniques can

The associate editor coordinating the review of this manuscript and approving it for publication was Xijun Wang.

help to improve the reliability by transmitting duplicated packets through multiple connected paths, or by sending divided portions of a file simultaneously through the multiple paths connecting the source and destination nodes [12]. Considering these two multipath transmission types, multipath transmission results in a trade-off between reliability and throughput based on how the multiple paths are used.

When a mobile device is connected over multiple heterogeneous networks, one of the most widely used protocols for multipath transmission is the multipath transmission control protocol (MPTCP). MPTCP can provide carrier aggregation that will enable higher throughput services by aggregating the bandwidth of multiple access networks (e.g., LTE and Wi-Fi) [6]. However, MPTCP requires kernel modification at both endpoints (client and server) [7], and there are still many middleboxes that do not allow MPTCP traffic to pass through [8].

In this paper, a multipath based adaptive concurrent transfer (MACT) scheme is proposed which supports application layer multipath data transfer via user datagram protocol (UDP) and also considers the status of the receiver buffer. The proposed scheme provides a method to satisfy QoE constraints as much as possible using adaptive control techniques to enhance the data rate or reliability according to the amount of frames in the buffer, the video encoding rate, priority of the frame, and the wireless network condition. The novelties of the proposed MACT scheme can be summarized as follows.

- MACT adaptively switches between two transmission schemes, fast concurrent transfer (FCT) and reliable concurrent transfer (RCT), to maximize the transmission rate and reliability.
- The stochastic models for FCT and RCT are derived considering the overall delay, frame size, packet loss rate, and the encoding video rate, which are used in the estimation process of the adaptation control scheme.
- MACT considers the receiver buffer status and latency conditions of the interactive video streaming system.
- MACT makes control decisions based on the frame characteristics and network conditions in situations where not all constraints can be satisfied simultaneously.

II. RELATED WORKS

Video streaming research using multipath transmission techniques have received much attention recently. Iyengar *et al.* [9] note that there were problems with multipath transmission, which include unnecessary fast retransmissions by the sender, window growth at the sender, and an increased number of acknowledgment messages (ACKs) due to fewer delayed ACKs returned from the receiver. The authors propose a solution that uses concurrent multipath transfer (CMT) based on the stream control transmission protocol (SCTP). Lee *et al.* [10] propose a technique to increase the fast retransmission threshold on the sender side to increase the performance of transmission control protocol (TCP) based on multipath techniques using a modified delayed ACK at the receiver. The proposed TCP based transmission scheme controls the window size based on received ACKs. In [11], a partial reliability based real-time streaming (PERES) UDP multipath transmission scheme is proposed, which considers ACKs and negative ACKs (NAKs) with buffer control of the receiver and sender to overcome delay constraints and reliability issues in video streaming over wireless networks. In [12], a forward error correction (FEC) based scheme that divides packets into multiple subpackets to minimize packet loss over multipath routing is proposed.

In [13], an offloading by restriction (OBR) scheme is proposed to improve the throughput by optimal data offloading when using two paths (5G and LTE) simultaneously. The proposed OBR scheme considers compatibility with MPTCP, where the congestion control and scheduling algorithm of MPTCP are applied in OBR. In [5], [14], and [15], the analysis results on MPTCP indicate that there is a trade-off between the energy consumption and received video quality, where the authors suggest methods for energy optimization in MPTCP. In [5], an energy distortion-aware MPTCP (EDAM) scheme is proposed to provide quality-guaranteed video streaming with improved energy-efficiency. EDAM considers energy consumption minimization through a video flow rate allocation algorithm based on an analytic energy distortion framework. In [14], an energy quality aware bandwidth aggregation (ELBA) scheme is proposed which supports energy-efficient bandwidth aggregation based on the delay and quality constraints in wireless networks. In [15], to achieve the target video quality with minimum device energy consumption, an energy-video aware multipath transport protocol (EVIS) is proposed.

III. SYSTEM MODEL

Because UDP is a connectionless transmission scheme with very low overhead, it is a very efficient transport protocol at the expense of lacking retransmission based reliability control. Compared to UDP, TCP is a connection-oriented slower transmission protocol, but supports retransmission based reliability and congestion control [16]. In this paper, the proposed MACT scheme adaptively combines the higher throughput benefits of UDP and the reliability features of TCP. MACT conducts real-time video transmission using UDP with data sequence mapping and duplicated ACK transmissions over multipath routed networks.

In this paper, the video codec used to encode and decode the real-time video is H.264 [17], where the encoded video rate is r kbps, and the video data consists of a group of pictures (GOP) which consists of F frames. It is also assumed that a GOP consists of one I frame and $(F - 1)$ P (or B) frames, where I frames are independently encoded pictures and P frames depend on one previously decoded I or P frame. P frames contain the motion-compensated differences (i.e., relative information) of other frames to achieve higher video compression rates. Therefore, I frames are more important than P frames, where the loss of an I frame is more critical to the video's QoE. It is assumed that an I frame and P frame are composed of Φ_I and Φ_P packets, respectively, and the average length of a packet constituting a frame is assumed to be L bits. It is also assumed that there are M paths between the video sender and receiver, which the transmission path is numbered as index m ($1 \leq m \leq M$), and the data rate of path m is d_m ($d_1 \geq \cdots \geq d_M$). In addition, the PLR of path m is expressed as π_m. In this paper, it is assumed that each path is independent of each other, therefore, they do not affect each other. In addition, corresponding to realistic network situations, each channel state is influenced by the PLR and the data rate changes according to time and various environmental factors. In this paper, it is assumed that the PLR and data rate are obtained through periodic monitoring of the channel state, and the monitoring period can be changed according to the user's speed, policy, application characteristics, and user density.

The proposed MACT system monitors the PLR, queueing delay, and data rate of each subflow between the source and destination. The end-to-end PLR of each path can be calculated by counting the number of received ACKs and the number of transmitted packets. It can be assumed that the minimum RTT over time is the RTT without queueing delay. Therefore, the lowest RTT record of a path can be considered as the path's transmission delay based RTT value. By subtracting a path's lowest RTT record from its current RTT value, the path's current queueing delay can be estimated. The queueing delay that occurs in each subflow can be estimated by monitoring the RTT of each path. In multipath communications, each path experiences a different delay resulting in different packet arrival times, which can cause problems.

MACT sends selective ACKs based on the data sequence mapping of MPTCP [18], which provides a subflow sequence for each path and a data sequence for the application-level. Packets sent through each multipath are stored and reordered based on the data sequence in the receiver buffer. Data sequence mapping associated segments are sent over different paths with data sequence numbering, so that segments can be reordered at the receiver buffer. It is determined that the transmission of the packet is successful if the data sequence is successfully transmitted over any subflow. On the other hand, it is assumed that the packet is lost if both the data and subflow sequence are out of order. In addition, if the ACK for the data sequence reception does not reach all paths, it is determined that the packet is lost even though the retransmission timeout (RTO) has not been exceeded. The description of parameters used in this paper are listed in Table 1.

TABLE 1. Parameter descriptions.

Parameters	Description
r	Encoded video rate
F	Number of frames which consists a GOP
Φ_I	Number of packets which consists an I frame
Φ_P	Number of packets which consists a P frame
L	Average length of a packet
M	Number of transmission paths between sender and receiver
m	mth multipath among the M multipaths
d_m	Average data rate of path m
π_m	Average packet loss rate (PLR) of path m
$n_{FCT,m}$	Ratio of packets transmitted through path m using fast concurrent transfer (FCT)
d_{FCT}	Throughput when transmitting based on FCT
R_{FCT}	Frame loss rate (FLR) when transmitting based on FCT
D_{FCT}	Round trip time (RTT) when transmitting based on FCT
$n_{RCT,m}$	Ratio of packets transmitted through path m using reliable concurrent transfer (RCT)
d_{RCT}	Throughput when transmitting based on RCT
R_{RCT}	FLR when transmitting based on RCT
D_{RCT}	RTT when transmitting based on RCT

IV. MULTIPATH BASED ADAPTIVE CONCURRENT TRANSFER ANALYSIS

A. MULTIPATH BASED CONCURRENT TRANSFER

In this paper, FCT and RCT are proposed as the simultaneous transmission methods used in MACT. Fig. 1 shows an overview of the multipath based FCT and RCT. In Fig. 1, two paths are connected between the source node and the destination node, and a frame composed of three packets (P1, P2, and P3) is transmitted. Fig. 1 (a) shows the outline of FCT, which aims to maximize the data rate by transmitting the largest number of packets in the shortest period of time. In Fig. 1 (a), P1 and P2 are transmitted through path 1, with subflow sequences 1 and 2, respectively, and P3 is transmitted through path 2, with subflow sequence 1. In Fig. 1, $T_m = L/d_m$, $T_{prop,m}$, and $T_{proc,m}$ are respectively the statistical transmission delay, propagation delay, and processing delay of path m. It is assumed that $T_{prop,m}$ is the same for data and ACK packets, and T_{ACK} is the transmission time consumed in transmitting an ACK packet at the destination node.

FCT intends to enhance the multipath concurrent transfer rate by controlling the last packet (of a frame) of the slower path to be transmitted before the last packet of the fastest path, in order to compensate for the time differences in the path delay. In Fig. 1 (a), P3,1 is completed before P2,2 is completed through path 1. When a frame is transmitted through FCT considering packet loss, the data rate d_{FCT} of FCT that considers packet loss can be expressed as

$$\text{maximize } d_{FCT} = \frac{(1 - R_{FCT})\Phi L}{D_{FCT}} \tag{1}$$

$$\text{subject to } D_{FCT} = \max\left(D_{FCT,1}, D_{FCT,2}, \cdots, D_{FCT,M}\right) \tag{2a}$$

$$R_{FCT} = 1 - \prod_{\phi=1}^{\Phi}\prod_{m=1}^{M}\left(1 - \pi_{\phi,m}\right) = 1 - \prod_{m=1}^{M}\left(1 - \pi_{\phi,m}\right)^{n_{FCT,m}\Phi} \tag{2b}$$

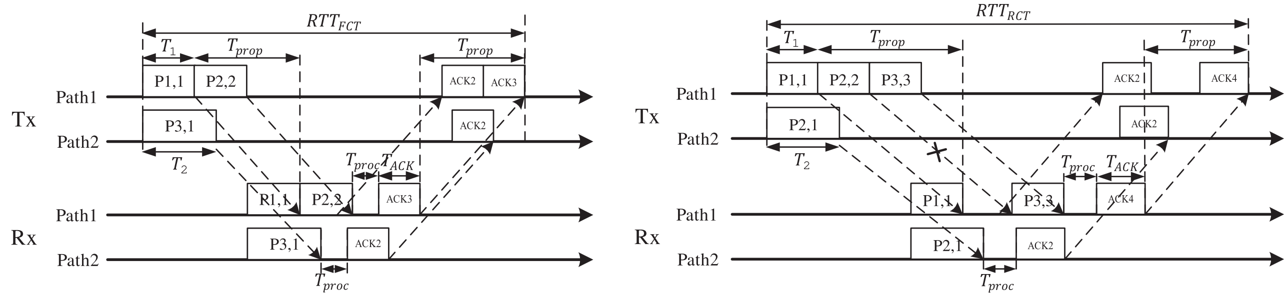

(a) Fast Concurrent Transfer (b) Reliable Concurrent Transfer

FIGURE 1. Multipath concurrent transfer examples of (a) FCT and (b) RCT.

$$\sum_{m=1}^{M} n_{FCT,m} = 1 \tag{2c}$$

where $n_{FCT,m}$ is the ratio of packets transmitted through path m, Φ is the average number of packets per frame, D_{FCT} is the round trip time (RTT) of FCT, $\Phi = \Phi_I$ for an I frame and $\Phi = \Phi_P$ for a P frame, and d_{FCT} represents the throughput when using automatic retransmission request (ARQ). Equation (2a) defines the RTT when one frame is transmitted through FCT based on UDP. In (2a), $\max\left(D_{FCT,1}, \cdots, D_{FCT,M}\right)$ refers to the delay of the slowest path, where $D_{FCT,m}$ is the RTT of path m based on FCT, and $(1 - R_{FCT})$ in (1) is the probability that all packets that make up the frame are successfully transmitted, where R_{FCT} in (2b) is the frame loss rate (FLR) of FCT.

Lemma 1: Assuming that Q_m is the queuing delay of path m, the packet transmission rate of each path is determined as $n_{FCT,1} : n_{FCT,2} : \cdots : n_{FCT,M} = \frac{Q-Q_1}{T_1} : \frac{Q-Q_2}{T_2} : \cdots : \frac{Q-Q_M}{T_M}$, where Q is the normalization constant to make $\sum_{m=1}^{M} \frac{Q-Q_m}{T_m} = \Phi$ in FCT.

Proof: In order to satisfy (1), a complicated and long-lasting algorithm (such as a heuristic algorithm) is required, which limits the difficulty in satisfying the fluctuating channel conditions and real-time characteristics of the service. Therefore, the semi-optimal value is derived by simplifying the equation. That is, it is assumed that (1) is satisfied through minimization of (2a) based on (3)

$$\begin{aligned} \text{minimize } D_{FCT} &= \max\left(D_{FCT,1}, D_{FCT,2}, \cdots D_{FCT,M}\right) \\ &\simeq \max\left(\Phi n_{FCT,1} T_1 + Q_1, \cdots \right. \\ &\qquad \left. , \Phi n_{FCT,M} T_M + Q_M\right) \end{aligned} \tag{3}$$

where RTTs of each subflows are statistically monitored, which are consisted of transmission, queueing, propagation, and processing delay along the multi-hop path. However, propagation and processing delay do not have much effect compared to the others. Assuming that the RTT without queuing delay is the minimum RTT over time, Q_m, which is the access link queuing delay of path m, can be estimated based on the RTT measured by the receiver, the transmission delay T_m, and $\Phi n_{FCT,m}$ [19]. It is assumed that path m' is the slowest path, which $\Phi n_{FCT,m'} T_{m'} + Q_{m'} \geq \Phi n_{FCT,m} T_m + Q_m$ for $\forall m$. Then, to minimize the maximum RTT, the slowest path m' tries to decrease the allocated packets $n_{FCT,m'}$ to lower its RTT until m' is no longer the slowest path. If this process is repeated, the RTT of each path becomes equal in the end as $n_{FCT,1} T_1 + Q_1/\Phi = \cdots = n_{FCT,M} T_M + Q_M/\Phi$. Therefore, the ratio of the packets allocated to each path is $n_{FCT,1} : n_{FCT,2} : \cdots : n_{FCT,M} = \frac{Q-Q_1}{T_1} : \frac{Q-Q_2}{T_2} : \cdots : \frac{Q-Q_M}{T_M}$, where Q is the normalization constant to make $\sum_{m=1}^{M} \frac{Q-Q_m}{T_m} = \Phi$. ∎

On the other hand, RCT is a transmission scheme that ensures reliability by transmitting the same packet through multiple paths. RCT consists of a main path and multiple backup paths. The main path transmits all data constituting the video stream frame, while other backup paths copy only partial data of the frame. Therefore, even if some data of the main path is lost or erroneous, duplicated packets transmitted through the backup path can be secured. In Fig. 1 (b), P1, P2, and P3 are transmitted through path 1, with subflow sequences 1, 2, and 3, respectively, and the duplicated P2 is transmitted through path 2, with subflow sequence 1. In Fig. 1 (b), P2 does not require additional retransmissions even though it fails to be delivered via path 1, because P2 is simultaneously transmitted through path 2. In Path 1, when P3,3 arrives, P2,2 does not arrive and "ACK2, SACK3" needs to be included in the ACK message. However, since P2 is transmitted through Path 2, the receiver transmits ACK4. RCT transmits all packets through the fastest path as well as through other paths simultaneously, where the RCT scheme determines the number of packets to be transmitted through the slower paths so that the throughput is kept the same as the throughput d_{RCT} of the fastest path even when errors occur. It is challenging to obtain an improvement in throughput when using RCT, but the reliability can be greatly increased through the transmissions of duplicated packets through multiple paths, where the FLR can be expressed as

$$\text{minimize } R_{RCT} = 1 - \prod_{\phi=1}^{\Phi} \left(1 - \prod_{m=1}^{M} x_{\phi,m} \pi_m\right) \tag{4}$$

subject to

$$d_{RCT} = \frac{(1-R_{RCT})\Phi L}{D_{RCT}} \tag{5a}$$

$$D_{RCT} = \max\left(D_{RCT,1}, D_{RCT,2}, \cdots D_{RCT,M}\right) = \Phi T_1 + Q_1 \tag{5b}$$

$$x_{\phi,1} = 1 \tag{5c}$$

$$x_{\phi,m} = \{1/\pi_m, 1\} \quad \text{where} \quad m \neq 1 \tag{5d}$$

where $x_{\phi,m}$ is 1 if packet ϕ is transmitted through path m, and $1/\pi_m$ if it is not sent through path m. D_{RCT} is the RTT of RCT, where $D_{RCT,m}$ is the RTT of path m based on RCT. A packet loss in RCT occurs when all of the duplicated packets fail to be delivered to the destination. Like in FCT, in RCT the rate of packets transmitted on each path $n_{RCT,m}$ is determined so that all packets complete transmission before transmission of the last packet (of the frame) on the fastest path is transmitted.

Lemma 2: The average number of paths that transmit each packet in RCT is $\sum_{m=1}^{M} \frac{d_m}{d_1} - d_m(\frac{Q_m - Q_1}{L\Phi})$.

Proof: In (5b), RTT due to each path does not exceed D_{RCT}. Therefore, if the rate of packets transmitted on each path is $n_{RCT,2}, n_{RCT,3}, \cdots, n_{RCT,M}$ $(0 \leq n_{RCT,m} \leq 1)$, the number of packets that can be transmitted on path m must satisfy the following equation.

$$\Phi T_1 + Q_1 \geq \Phi n_{RCT,m} T_m + Q_m \tag{6}$$

Therefore, $n_{RCT,m} \leq d_m/d_1 - d_m((Q_m - Q_1)/L\Phi)$ should be satisfied. The total possible number of packets transmitted is $\sum_{m=1}^{M} \Phi n_{RCT,m} \simeq \sum_{m=1}^{M} \Phi(\frac{d_m}{d_1} - d_m(\frac{Q_m - Q_1}{L\Phi})))$ and the transmission path of each packet is distributed as evenly as possible. Then, the average number of transmission paths of each packet is represented as $\sum_{m=1}^{M} \frac{d_m}{d_1} - d_m(\frac{Q_m - Q_1}{L\Phi})$. ∎

After frame transmission is completed, both FCT and RCT send a report on the lost packet through the returned ACK. In Fig. 1 (b), even if delivery failure of P2 is detected on path 1, an ACK is not transmitted instantly. Instead, after all packets of the frame have been received, an ACK is sent in regards to the erroneous packet(s). The data rate d_m and FLR R_m of each path is also reported back to the source node.

B. MACT CONTROL SCHEME BASED ON RECEIVER BUFFER STATUS

In wireless networks, discontinuity of playback may occur due to various factors, such as, sudden channel state change, traffic congestion, and packet loss. These factors cause serious degradation in user QoE. The number of frames in the receiver buffer varies with time. If packets are delayed, the buffer may become underflow, where there is not enough data in the buffer to support a continuous playback. In such cases, stalling in the video play can occur. On the other hand, if a large amount of traffic is rapidly entering the buffer, buffer overflow may occur. In this case, packets that arrive after the buffer is full will be lost. Therefore, it is important to keep the number of frames in the receiver buffer to a certain level to maintain high service quality. In this section, a MACT scheme is proposed which maintains the number of frames in the buffer at a certain level by controlling the ratio of FCT and RCT and deciding when to use retransmission.

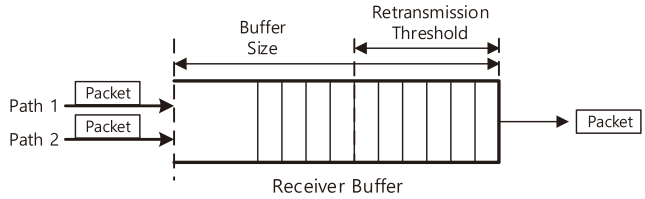

FIGURE 2. Receiver buffer overview.

The proposed MACT scheme conducts adaptive concurrent transmission based on the amount of frames in the destination's buffer. The MACT scheme requires the receiver buffer to conduct packet ordering to compensate for arrival time differences of packets through the different paths. Fig. 2 presents a schematic diagram of the receiver buffer that receives packets through two paths. The size of the receiver buffer depends on the time constraint H s of the streaming service [20]. Therefore, the end-to-end delay between transmission and playback are set to not exceed H s.

$$\frac{F_B \Phi L}{r} + \frac{\Phi L}{\min\{d_{RCT}, d_{FCT}\}} + T_{prop} + T_{proc} \leq H \tag{7}$$

The maximum number of frames in the buffer F_B is set to satisfy the above inequality, which is based on the size of the buffer B. The retransmission threshold θ is set to its maximum possible value considering F_B such that retransmission can be conducted without experiencing any stalling during real-time video streaming. That is, retransmission is not conducted from the first frame to the θth frame in the buffer to prevent playout stalling because the delay due to retransmission is longer than the time remaining until the playback.

The state of the buffer is classified into four cases according to the number of frames in the buffer F_B and the buffer level increment rate. In Fig. 3, case 1 occurs when F_B does not exceed θ and continues to decrease, case 2 occurs when F_B does not exceed θ but continues to increase, case 3 occurs when F_B exceeds θ and continues to increase, and case 4 occurs when F_B exceeds θ but continues to decrease.

If case 1 continues (Fig.3 (a)), playout stalling will occur once the buffer empties, therefore the destination node needs to enter case 2 to prevent this from happening. Therefore, it is required to improve the throughput through the following policy for the GOPs that are being transmitted

$$\text{minimize} \;\; R = \frac{\alpha R_{RCT} + (F-\alpha) R_{FCT}}{F} \tag{8}$$

$$\text{subject to} \; d = \frac{\alpha d_{RCT} + (F-\alpha) d_{FCT}}{F} > r \tag{9}$$

where α is the number of frames transmitted using RCT in the GOP. The MACT scheme needs to apply an α that minimizes the FLR while increasing the throughput above the encoding rate r. In this case, (8) and (9) are monotonously decreasing linear functions in a weighted sum

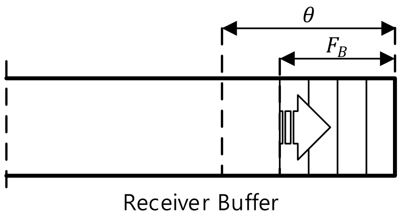

(a) case 1

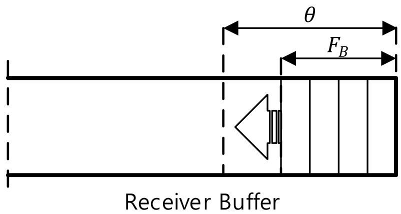

(b) case 2

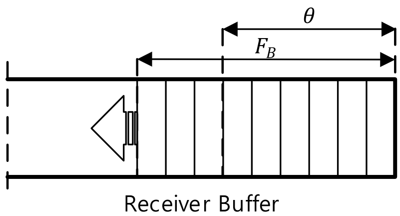

(c) case 3

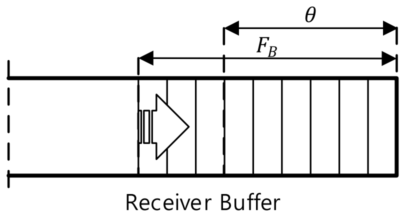

(d) case 4

FIGURE 3. State cases of the receiver buffer.

form, and $\alpha_{UB} = F(d_{FCT} - r)/(d_{FCT} - d_{RCT})$ satisfies (8). If case 2 conditions continue, the status may change to case 3, where the buffer will become full and packets may be dropped due to buffer overflow. In this condition, enhancing the throughput will no longer provide QoE improvements. If this status continues, the status may change to case 4 through the following policy to improve the system reliability,

$$\text{maximize } d = \frac{\alpha d_{RCT} + (F-\alpha)d_{FCT}}{F} \tag{10}$$

$$\text{subject to } R = \frac{\alpha R_{RCT} + (F-\alpha)R_{FCT}}{F} \leq R_C \tag{11}$$

where R_C is the reliability constraint of the service. In contrast to the control statement of (8), control policy (10) maximizes the data rate under the constraint of keeping the FLR condition, where the optimal α value is searched to satisfy the objective function (10). Policy (10) and (11) are respectively modified versions of (8) and (9), where the constraint condition is changed to $\alpha_{LB} = F(R_{FCT} - R_C)/(R_{FCT} - R_{RCT})$. When in case 4 and (10) is applied, entry into case 1 occurs, which hopefully can be maintained until the video streaming is completed. Using the control statements (8) and (10), the range of α based on a GOP will be $F(R_{FCT} - R_C)/(R_{FCT} - R_{RCT}) \leq \alpha \leq F(d_{FCT} - r)/(d_{FCT} - d_{RCT})$. Frames with higher priority (according to the video encoding policy) can be serviced through RCT to enhance the reliability.

The proposed MACT scheme can be implemented with or without priority support for the packets of I frames. The reason that higher priority support for I frames (compared to P and B frames) could be beneficial to the performance in poor network conditions is because an error event occurring to an I frame can result in consecutive P and B frame decoding failures [11]. One consideration is that, because I frames are larger compared to P and B frames, more packets are needed to transfer an I frame. The proposed MACT scheme can be configured to apply RCT to all packets of an I frame when degraded network conditions are detected. In addition, the proposed MACT scheme can be configured to consecutively stream all packets of an I frame and use an accumulated ACK for the packets to reduce the frequency of ACKs. If needed, accumulated ACK transmission can be applied to the packets corresponding to a P or B frame as well. For example, in H.264, the importance of an I frame is higher than a P frame, so for an I frame $\alpha \geq 1$ can be set such that I frame transmissions are conducted in RCT. In addition to I frames, packets with high priority will be subject to RCT support, which include packets used for control of real-time services. RCT can also be used for erroneous packet retransmission, which can be quickly detected through the control plane that is monitoring the error events in the network and physical layers.

MACT has partial reliability characteristics according to the buffer case classification, which has some relevance to the partial reliable SCTP (PR-SCTP). PR-SCTP is proposed by the IETF for real-time multimedia [21], which can support varying reliability levels by stopping data retransmission before a certain transmission sequence number (TSN). On the other hand, MACT can maintain a target reliability level while minimizing data traffic of the stream by controlling the ratio between FCT and RCT and the buffer state.

C. MACT ALGORITHM

The pseudocode of the MACT scheme is presented in Algorithm 1. MACT uses GOP size F, encoding rate r, Φ_I, Φ_P, and L as input. When preparing for video streaming, the receiver's buffer size and θ is calculated based on the input information (step 1) and the initial value of α is set to 1 for reliable I frame transmission (step 2).

During video streaming (step 3), the current status is classified according to the number of frames in the buffer F_B and

Algorithm 1 MACT Algorithm

input r, Φ_I, Φ_P, L
1: **compute** buffer size B and θ
2: **set** $\alpha = 1$ for reliable I frame transfer
3: **for** *video streaming* **do**
4: **get** throughput and PLR of each path
5: **if** $f_B \leq \theta$ **then**
6: **if** case 1: $d \leq r$ **then**
7: **apply** the policy of case 1 using (8)
8: **else** case 2:
9: **maintain** the policy of case 1
10: **end if**
11: **else**
12: **if** case 4: $d \leq r$ **then**
13: **maintain** the policy of case 3
14: **else** case 3:
15: **apply** the policy of case 3 using (10)
16: **end if**
17: **end if**
18: **end for**

throughput d. When in case 1 status, the control condition of (8) is applied to increase the number of frames transmitted through FCT (steps 5, 6, and 7). When in case 2 status, the control condition of (7) is maintained (step 5, 8, and 9). If a transition from case 2 to case 3 occurs, the ratio of RCT is increased based on (9) (step 11, 12, and 13). If case 4 status is entered, the control condition of (10) is maintained (step 11, 14, and 15). This continues until the video streaming is complete.

V. PERFORMANCE ANALYSIS

In the video streaming performance analysis, the time limit H is set to 150 ms [20] and it is assumed that H.264 GOPs consist of an average of one I frame and nine P frames (i.e., $F = 10$) with an average packet size L of 1400 bytes. The streaming video used in the experiment is a 1080p (1920×1020) HD video with 30 fps at an encoding rate of 8 Mbps. It is assumed that there are two paths between the video provider (source node) and receiver (destination node), where one path goes through the cellular network and the other path is connected through Wi-Fi. Performance analysis is conducted by comparing MACT with MPTCP, TCP, and PERES, which is an UDP transmission method considering ACK/NAK and buffer control [11].

The data rate and PLR of path 1 and path 2 are respectively assumed to be 8 Mbps and 0.02, and 5 Mbps and 0.06. Fig. 4 (a) presents the average throughput graph for the video frames. In Fig. 4 (a), MACT and MPTCP have an average throughput of 9.10 Mbps and 8.37 Mbps, respectively, which fully satisfies the video rate requirement of 8 Mbps. The throughput of TCP and PERES are respectively 8.25 Mbps and 8.24 Mbps, which also satisfy the video rate requirement when the channel condition is good. Fig. 4 (b) presents the

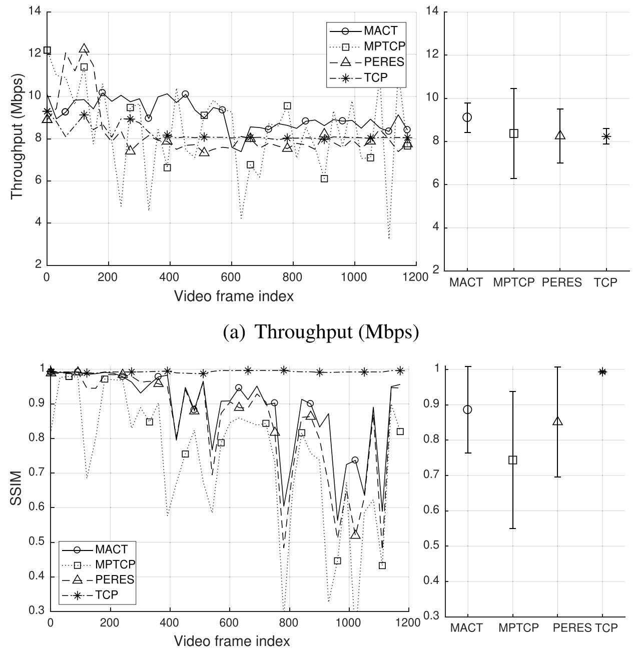

(a) Throughput (Mbps)

(b) SSIM

FIGURE 4. **Video quality in good channel conditions.**

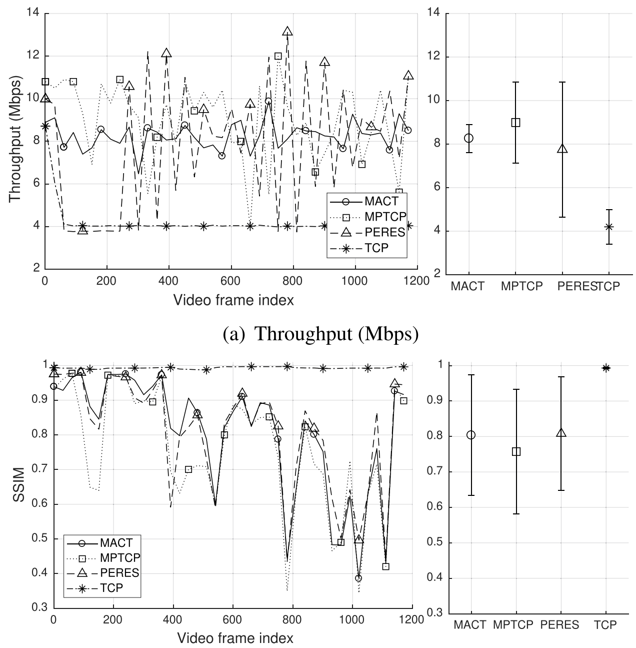

(a) Throughput (Mbps)

(b) SSIM

FIGURE 5. **Video quality in bad channel conditions.**

performance graph of structural similarity (SSIM) of a video streaming image through each transmission technique compared to its original video image [22]. In Fig. 4 (b), the SSIM of UDP-based MACT and PERES are 0.88 and 0.84, respectively, which are higher than the SSIM of MPTCP, 0.74. While the SSIM of TCP is about 1, the SSIM of MPTCP

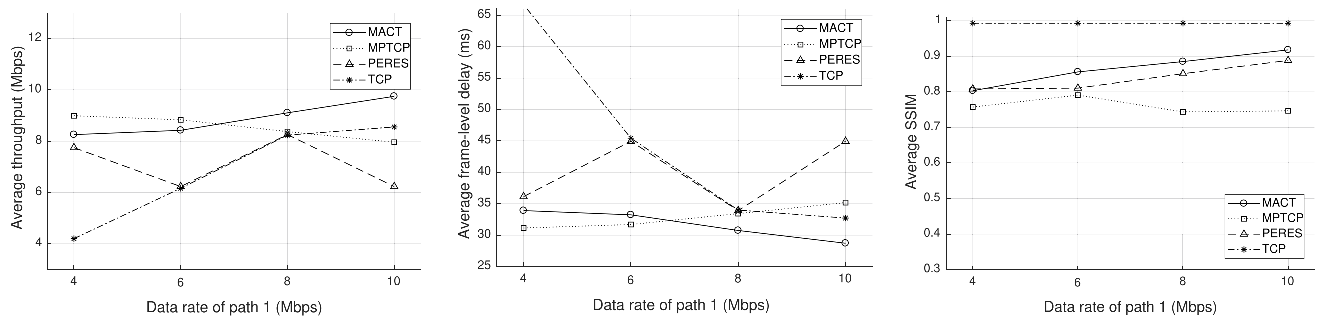

(a) Average throughput (b) Average frame-level delay (c) Average SSIM

FIGURE 6. Influence of channel data rate changes.

is 0.74, which can be caused by lack of consideration of the receiver buffer. The results of Fig. 4 (a) and (b) demonstrate that TCP and PERES over a single path can result in a good performance, when the main path has a sufficiently good channel condition.

Then, while maintaining the characteristics of path 2, the data rate of path 1 is lowered to be 4 Mbps and PLR of 0.02 under poor channel conditions. Fig. 5 (a) and (b) present the performance graph of throughput and SSIM, respectively, when the data rate of path 1 is lowered to 4 Mbps while the PLR is still 0.02. In Fig. 5 (a), MACT and MPTCP have an average throughput of 8.25 Mbps and 8.99 Mbps, respectively, which still satisfy the video rate requirement of 8 Mbps. However, the throughput of PERES and TCP are respectively 7.74 Mbps and 4.20 Mbps, which cannot satisfy the video encoding rate requirement. In addition, the standard deviation of PERES is the largest value of the four that are compared, 3.09 Mbps, which may cause a drop in QoS due to the fluctuation of PERES. In Fig. 5 (b), the SSIM of UDP-based MACT and PERES are 0.80 and 0.80, respectively, which are higher than the SSIM of MPTCP, which is 0.75. TCP can provide a high SSIM value at the cost of having the lowest throughput performance among the four compared, which is why it would be unsuitable to apply TCP in real-time video streaming networks that experience packet delivery failures. The results of Fig. 5 (a) and (b) demonstrate that MACT can provide a better performance compared to MPTCP, PERES, and TCP, when the main path has a low data rate.

Fig. 6 shows that the video quality changes according to the data rate of the channel. In Fig. 6, MACT and MPTCP have a higher throughput and lower frame-level delay than the encoding rates regardless of the changes in the data rate of path 1, and that MACT can provide a higher SSIM than MPTCP. While TCP continues to show a high SSIM (about 1), it can be seen that the frame-level delay is the highest when the data rate is low. The SSIM of PERES increases as the data rate increases, but PERES shows a low throughput performance when the data rate of path 1 is low, which is similar to TCP.

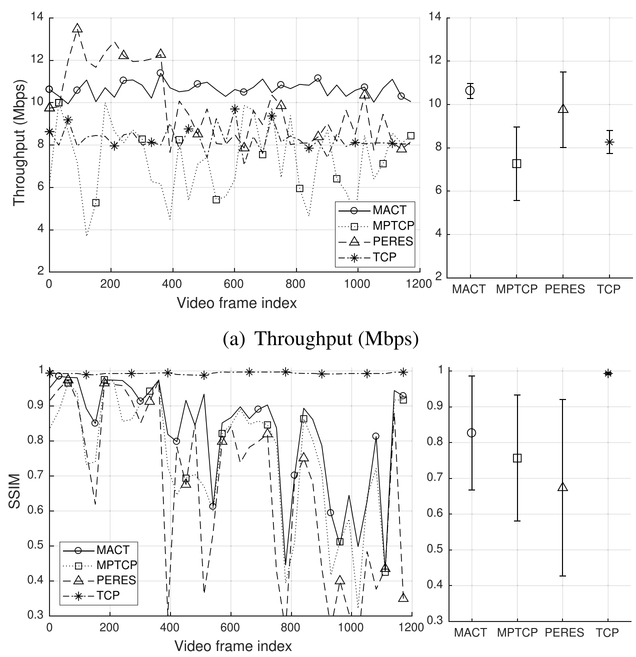

(a) Throughput (Mbps)

(b) SSIM

FIGURE 7. Video quality in erroneous channel conditions.

When the data rate of path 1 is 8 Mbps and the PLR is 0.05, Fig. 7 (a) and (b) present the performance graph of the throughput and SSIM, respectively. In Fig. 7 (a), MACT has an average throughput of 10.63 Mbps, which is the largest and most stable. The throughput of MPTCP and TCP (i.e., 7.27 Mbps and 8.26 Mbps, respectively) are lower than MACT and PERES (i.e., 10.63 Mbps and 9.76 Mbps, respectively), which is due to the window size reduction effect when lost packets are detected. In Fig. 7 (b), the SSIM of multipath-based MACT and MPTCP are 0.82 and 0.75, respectively, which are higher than the SSIM of PERES, 0.67, which is a single path UDP based transmission scheme.

Fig. 8 shows the video quality changes based on the channel error rate. When the data rate is the same and PLR

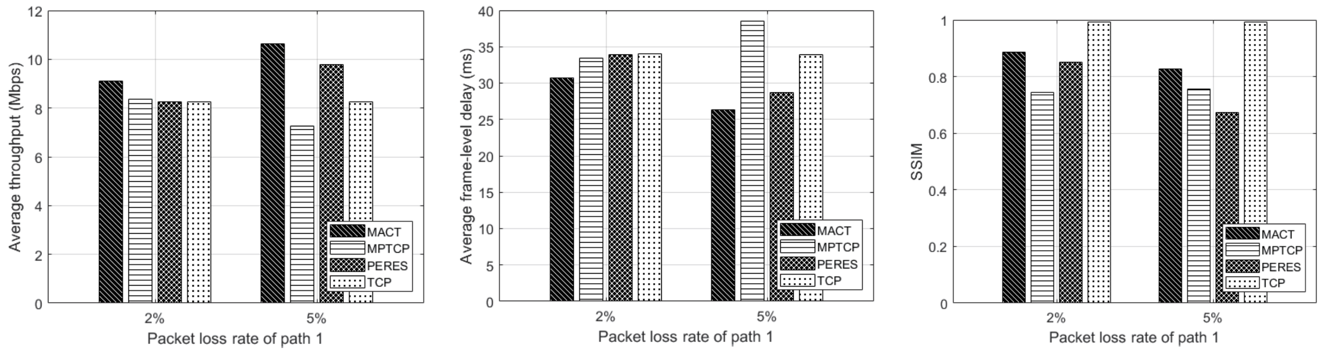

(a) Average throughput (b) Average frame-level delay (c) Average SSIM

FIGURE 8. **Influence of PLR.**

is changed from 2% to 5%, MACT shows no significant change or only a slight improvement in throughput, frame-level delay, and SSIM, while the throughput of MPTCP decreases and the frame-level delay of MPTCP increases. In addition, the SSIM of PERES is significantly reduced. Based on Fig. 6 and Fig. 8, if the primary path maintains good channel conditions, the performance of TCP and PERES over a single path may be sufficient. However, if the data rate of the primary path drops or the PLR rises, resulting in poorer channel conditions, MACT is more stable and can provide a better performance than MPTCP, TCP, and PERES.

VI. CONCLUSION

In this paper, the MACT scheme is proposed, which is designed to provide higher levels of throughput and SSIM performance to enhance the QoE of real-time video streaming services using multipath networks that experience packet delivery failures. MACT uses adaptive switching of FCT and RCT mode based on the buffer level of the destination node, frame priority, and the multipath network conditions. The experiment results show that the MACT scheme can provide an improved real-time video streaming performance compared to MPTCP, PERES, and TCP over networks with poor channel conditions, which have low data rates or high PLRs.

REFERENCES

[1] 5G Infrastructure Association. (2015). *5G Automotive Vision*. [Online]. Available: https://5g-ppp.eu/wp-content/uploads/2014/02/5G-PPP-WhitePaper-on-Automotive-Vertical-Sectors.pdf

[2] V. Sharma, K. Kar, K. K. Ramakrishnan, and S. Kalyanaraman, "A transport protocol to exploit multipath diversity in wireless networks," *IEEE/ACM Trans. Netw.*, vol. 20, no. 4, pp. 1024–1039, Aug. 2012.

[3] Z. Duanmu, K. Zeng, K. Ma, A. Rehman, and Z. Wang, "A quality-of-experience index for streaming video," *IEEE J. Sel. Topics Signal Process.*, vol. 11, no. 1, pp. 154–166, Feb. 2017.

[4] I.-P. Belikaidis, A. Georgakopoulos, P. Demestichas, B. Miscopein, M. Filo, S. Vahid, B. Okyere, and M. Fitch, "Multi-RAT dynamic spectrum access for 5G heterogeneous networks: The SPEED-5G approach," *IEEE Wireless Commun.*, vol. 24, no. 5, pp. 14–22, Oct. 2017.

[5] J. Wu, B. Cheng, M. Wang, and J. Chen, "Quality-aware energy optimization in wireless video communication with multipath TCP," *IEEE/ACM Trans. Netw.*, vol. 25, no. 5, pp. 2701–2718, Oct. 2017.

[6] A. Ford, C. Raiciu, M. Handley, and O. Bonaventure, *TCP Extensions for Multipath Operation with Multiple Addresses*, document RFC 6824, 2013.

[7] C. Raiciu, C. Paasch, S. Barre, A. Ford, M. Honda, F. Duchene, O. Bonaventure, and M. Handley, "How hard can it be? Designing and implementing a deployable multipath TCP," in *Proc. 9th Symp. Netw. Syst. Design Implement.*, San Jose, CA, USA, vol. 2012, pp. 399–412.

[8] B. Hesmans, F. Duchene, C. Paasch, G. Detal, and O. Bonaventure, "Are TCP extensions middlebox-proof?" in *Proc. Workshop Hot Topics Middleboxes Netw. Function Virtualization*, Santa Barbara, CA, USA, Dec. 2013, pp. 37–42.

[9] J. R. Iyengar, P. D. Amer, and R. Stewart, "Concurrent multipath transfer using SCTP multihoming over independent end-to-end paths," *IEEE/ACM Trans. Netw.*, vol. 14, no. 5, pp. 951–964, Oct. 2006.

[10] Y. Lee, I. Park, and Y. Choi, "Improving TCP performance in multipath packet forwarding networks," *J. Commun. Netw.*, vol. 4, no. 2, pp. 148–157, Jun. 2002.

[11] J. Wu, R. Tan, and M. Wang, "Streaming high-definition real-time video to mobile devices with partially reliable transfer," *IEEE Trans. Mobile Comput.*, vol. 18, no. 2, pp. 458–472, Feb. 2019.

[12] S. Dulman, T. Nieberg, J. Wu, and P. Havinga, "Trade-off between traffic overhead and reliability in multipath routing for wireless sensor networks," in *Proc. IEEE Wireless Commun. Netw.*, New Orleans, LA, USA, Mar. 2013, pp. 1918–1922,

[13] C. Lee, S. Song, H. Cho, G. Lim, and J.-M. Chung, "Optimal multipath TCP offloading over 5G NR and LTE networks," *IEEE Wireless Commun. Lett.*, vol. 8, no. 1, pp. 293–296, Feb. 2019.

[14] J. Wu, B. Cheng, M. Wang, and J. Chen, "Energy-efficient bandwidth aggregation for delay-constrained video over heterogeneous wireless networks," *IEEE J. Sel. Areas Commun.*, vol. 35, no. 1, pp. 30–49, Jan. 2017.

[15] J. Wu, C. Yuen, B. Cheng, M. Wang, and J. Chen, "Energy-minimized multipath video transport to mobile devices in heterogeneous wireless networks," *IEEE J. Sel. Areas Commun.*, vol. 34, no. 5, pp. 1160–1178, May 2016.

[16] J. W. Overstreet and A. Tzes, "An Internet-based real-time control engineering laboratory," *IEEE Control Syst. Mag.*, vol. 19, no. 5, pp. 19–34, Oct. 1999.

[17] *Advanced Video Coding for Generic Audiovisual Services*, Standard ITU-T Recommendation H.264, May 2003.

[18] A. Ford, C. Raiciu, M. Handley, S. Barre, and J. Iyengar, *Architectural Guidelines for Multipath TCP Development*, document RFC 6182, Mar. 2011.

[19] H. Im, C. Joo, T. Lee, and S. Bahk, "Receiver-side TCP countermeasure to bufferbloat in wireless access networks," *IEEE Trans. Mobile Comput.*, vol. 15, no. 8, pp. 2080–2093, Aug. 2016.

[20] J. G. Apostolopoulos, W. Tan, and S. J. Wee, "Video streaming: Concepts, algorithms, and systems," HP Laboratories, Palo Alto, CA, USA, Tech. Rep. HPL-2002-260, Sep. 2002.

[21] R. Stewart, M. Ramalho, Q. Xie, M. Tuexen, and P. Conard, *Stream Control Transmission Protocol (SCTP) Partial Reliability Extension*, document RFC 3758, May 2004.

[22] Z. Wang, A. C. Bovik, H. R. Sheikh, and E. P. Simoncelli, "Image quality assessment: From error visibility to structural similarity," *IEEE Trans. Image Process.*, vol. 13, no. 4, pp. 600–612, Apr. 2004.

SOOEUN SONG received the B.S. degree from the School of Electrical and Electronic Engineering, Yonsei University, Seoul, South Korea, where he is currently pursuing the combined M.S. and Ph.D. degrees. He is currently a Research Member of the Communications and Networking Laboratory (CNL), Yonsei University. His research interests include NFV/SDN, MEC, 5G mobile systems, and URLLC.

JAEWOOK JUNG received the B.S. degree from the School of Electrical and Electronic Engineering, Yonsei University, Seoul, South Korea, where he is currently pursuing the combined M.S. and Ph.D. degrees in electrical and electronic engineering and also a Researcher of the CNL. His current research interests include 5G mobile systems and multipath TCP.

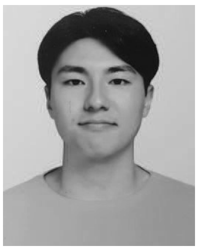

MINSU CHOI received the B.S. degree from the School of Electrical and Electronic Engineering, Yonsei University, Seoul, South Korea, where he is currently pursuing the combined M.S. and Ph.D. degrees in electrical and electronic engineering and also a Researcher of CNL. His research interests include 5G mobile systems, NFV/SDN, MEC, and URLLC.

CHANGSUNG LEE received the B.S. degree in electrical and electronic engineering from Yonsei University, Seoul, South Korea, in 2016, where he is currently pursuing the combined M.S. and Ph.D. degrees in electrical and electronic engineering and also a Researcher of CNL. His current research interests include 5G mobile systems, intelligent handover, and multipath TCP.

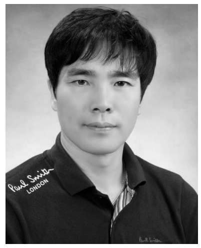

JUNGKYU SUN received the M.S. degree from the Department of Defense Fusion Engineering, Yonsei University, Seoul, South Korea, in 2019. He is currently a Team Manager with LIG Nex1 Company Ltd., Seongnam, Gyeonggi, South Korea. His research interests include military communication, multipath communication, and unmanned vehicle communications.

JONG-MOON CHUNG received the B.S. and M.S. degrees in electronic engineering from Yonsei University, and the Ph.D. degree in electrical engineering from Pennsylvania State University.

From 1997 to 1999, he was an Assistant Professor and an Instructor with the Pennsylvania State University. From 2000 to 2005, he was with Oklahoma State University (OSU), as a Tenured Associate Professor. Since 2005, he has been a Professor with the School of Electrical and Electronic Engineering, Yonsei University, where he is currently an Associate Dean with the College of Engineering.

He was a recipient of the First Place Outstanding Paper Award at the IEEE EIT 2000 Conference, Chicago, USA, in 2000, and the Technology Innovator Award and the Distinguished Faculty Award from OSU, in 2004 and 2003, respectively. As a Tenured Associate Professor with OSU, he was a recipient of the Regents Distinguished Research Award and the Halliburton Outstanding Young Faculty Award, in 2005, the Republic of Korea Government's Defense Acquisition Program Administration (DAPA) Award, in 2012, the Outstanding Teaching Awards from Yonsei University, in 2007, 2009, 2014, and 2019, and the Outstanding Accomplishment Faculty Awards, in 2008, 2018, and 2019. He was also a recipient of the Pledge Book Award of the Eta Kappa Nu (HKN). In addition, his 12 Coursera (www.coursera.org) courses are among the most popular, which focus on deep learning, big data, cloud computing, 5G & 4G mobile communications, Wi-Fi, Bluetooth, augmented reality (AR), the Internet of Things (IoT), Skype, YouTube, H.264, MPEG-DASH, TCP/IP, and the hardware and software of smartphones and smart watches. He was the General Chair of several conferences including IEEE MWSCAS 2011, and he will be serving as the General Chair of IEEE ICCE 2022 and IEEE ICCE-Asia 2020. He serves as the Vice President of the IEEE Consumer Electronics Society, an Editor of the IEEE Transactions on Vehicular Technology, an Associate Editor of the IEEE Transactions on Consumer Electronics, an Section Editor of the Wiley *ETRI Journal*, and an Co-Editor-in-Chief of the *KSII Transactions on Internet and Information Systems*.